Initiation and Development of the Heat-Affected Zone in the Vibration Welding of Polyvinylidene Fluoride and Its Copolymers

D. Valladares, M. Cakmak

Polymer Engineering Institute, College of Polymer Engineering and Polymer Science, University of Akron, Akron, Ohio 44325-0301

Received 20 July 2001; accepted 18 March 2002

ABSTRACT: Using a servo hydraulically controlled vibration-welding machine, the temporal and spatial development of hierarchical structure in the heat-affected zone of Poly(vinylidene fluoride) homopolymer and a copolymer of vinylidene fluoride and hexafluorpropylene are investigated. The dynamical changes early in the welding process are rather complex, and start at highly localized regions that then develop rapid adhesive character. In subsequent stages, these regions coalesce and a wave pattern establishes with wave normals oriented in the vibration direction. The crests of the waves near the side surfaces then begin to extrude fibrillar structure. These fibers are also collected and extruded in the vibration direction with their long axes normal to the vibration direction. The production of such features is partly attributed to the high melt elasticity of these polymers that results in instability resulting in their production. X-ray analysis indicates that the fibers are unoriented in their crystalline regions but electron microscopy studies show that a spiral orientation develops in the extruded fibers indicating that they underwent extension plus twisting deformation. © 2002 Wiley Periodicals, Inc. J Appl Polym Sci 86: 3377–3388, 2002

Key words: vibration welding; PVDF; welding development

INTRODUCTION

Large parts with complex geometry can be easily welded using vibration welding. This is one of the main advantages of this technique over other friction welding techniques such as spin and ultrasonic welding.[1–5] In addition, this process can be easily automated for mass production. This technique has been analyzed in several past studies. Stokes was the first to observe the four characteristic phases of the process in the penetration–time curves. He also developed a mathematical modeling for this process. Past studies on vibration welding primarily focused on evaluating mechanical properties of the welded parts as a function of the principal process parameters; frequency, amplitude, and pressure.[6–8] These studies include Polycarbonate (PC), Poly(butylene terephthalate) (PBT), Polyetherimide (PEI), and modified Poly phenylene oxide (M-PPO) and Polypropylene[9–11] nylon 6 and nylon 66.[12] In addition, the effect of glass fiber fillers on welding behavior of PBT[13] and nylon 6 and nylon 66 was studied.[14] There are some studies on vibration welding of dissimilar materials such as PC/PEI[15] and ABS to itself and to PC, PBT, PEI.[16] In the dissimilar joints the strength of PC, the weaker of the two materials could be attained. This strength is primarily determined by the mechanical interlocking at the weld interface caused by the mixing of molten layers of the two polymers by the shear action.

A study of structure development at the heat affected zone (HAZ) of vibration welded polyethylene naphthalate (PEN) parts by Cakmak, Robinette, and Schaible[17,18] found that the interface between the heat-affected region and unaffected region of amorphous PEN welds is not straight. Wave-like patterns were observed particularly at the interior regions. A secondary HAZ was found on either side of the main HAZ, which optically shows some level of deformation but did not crystallize during the welding stage. High levels of crystalline orientation with the chain axes oriented parallel to the weld plane in the direction of the vibration were observed in the interior of the HAZ. The naphthalene planes, roughly parallel to the weld interface, are detrimental to the mechanical properties and reduces the strength of the weld interface. A study of structure development and dynamics of vibration welding of PEN from amorphous and semicrystalline precursors by Cakmak, Robinette, and Schaible[18] showed significant differences in the welding behavior and resulting properties of PEN samples welded from amorphous or crystalline precursors. For the same process parameters, weld penetration started at shorter times in amorphous samples because of the lower temperature to reach T_g, while crystalline sam-

Correspondence to: M. Cakmak.

Journal of Applied Polymer Science, Vol. 86, 3377–3388 (2002)

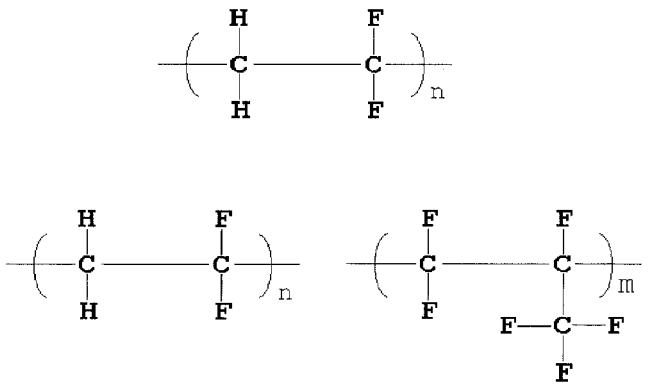

Figure 1 Repeat unit of PVDF homopolymer and copolymer.

ples remain solid until the temperature reach the start of the melting range, which is about 120°C higher. The samples welded from crystalline precursors shown orientation similar to the samples welded from amorphous precursor, but the orientation levels were found to be less, resulting in much higher weld strengths for the crystalline samples.

Polyvinylidene fluoride

Polyvinylidene fluoride (PVDF) is a polymer of —(CF_2—CH_2)— repeating unit. Commercial PVDF is obtained polymerizing vinylidene fluoride in a suspension or emulsion system; initiated by free radicals.[19] Crosslinking can be achieved by exposure to electron radiation. The main physical properties are the specific gravity (between 1.75 and 1.78 g/cm^3) and the refractive index of 1.42. This material is very resistant to strong acids, bases, and organic solvents, as well as environment factors such as temperature and UV radiation. It has good mechanical resistance, and it is able to support high levels of fatigue and abrasion. Therefore, PVDF is used in a wide range of applications, including coating, pipes, tanks, pumps, etc.

PVDF crystallizes from the melt in two different forms: form I (β) and form II (α). In addition, other forms have been found, such as form III (γ) and form IV (δ), which are obtained under specific processing conditions. The β form has an orthorhombic unit cell with a chain conformation *trans-trans* zig-zag plane. The α form contains a monoclinic unit cell with a *trans-gauche trans-gauche* conformation. The γ form is a combination of the previous forms presenting a monoclinic unit cell with a chain conformation *trans-trans* zig-zag plane. The PVDF crystalline percent is between 35 and 65%. The crystalline percent and the crystal structure are dependent of several factors, such as the thermal history of the material. PVDF presents high mold contractions (around 3%) due to its high crystalline levels.[19]

Much less information is available on the structural hierarchy developed in the heat-affected zone of vibration welded products that govern the mechanical

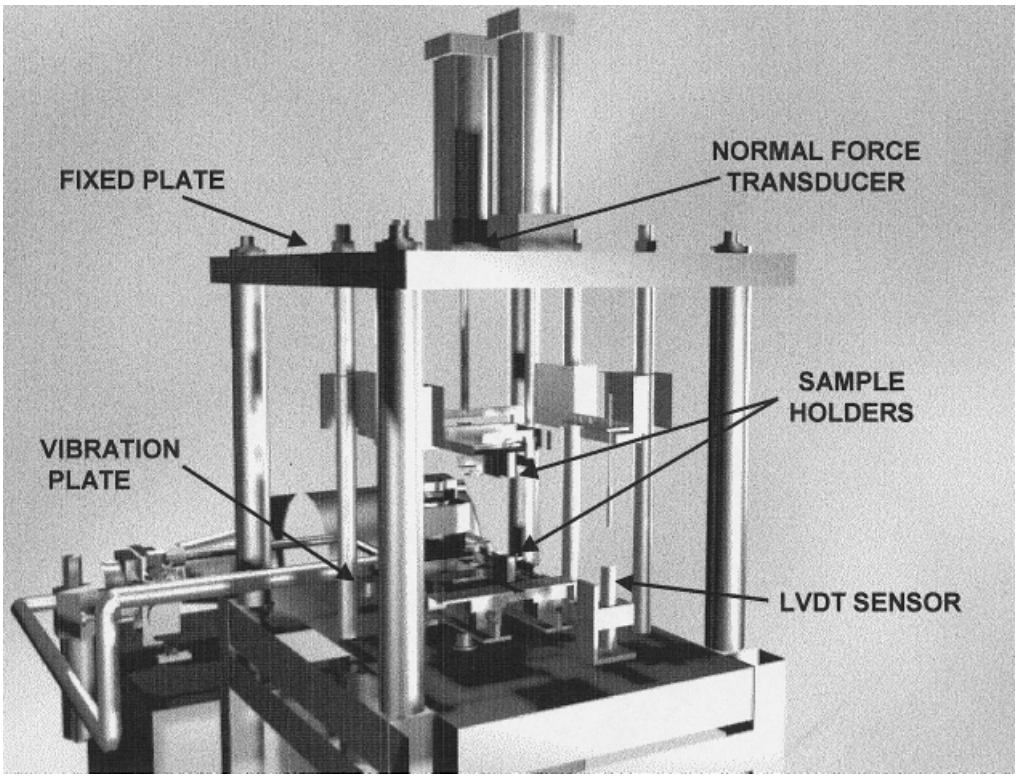

Figure 2 Instrumented vibration welding machine.

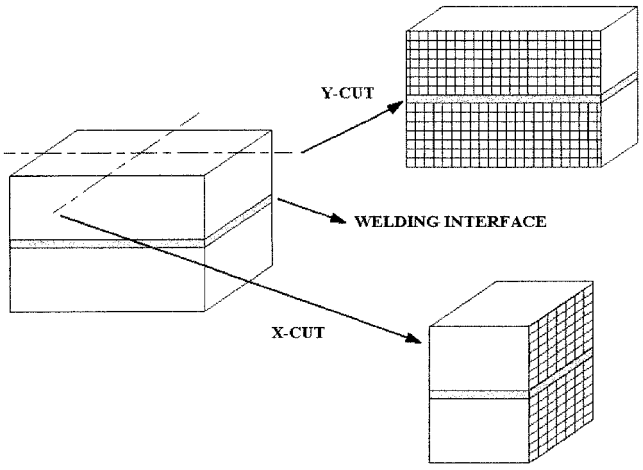

Figure 3 Sample cutting procedures.

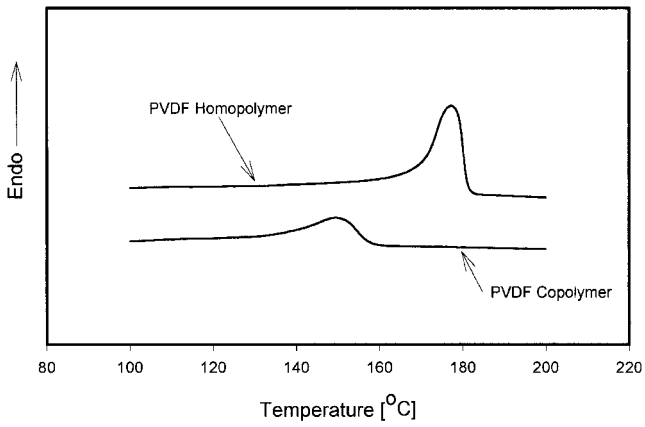

Figure 4 DSC scans on an as-received PVDF homopolymer and copolymer.

performance characteristics. The main issues particularly related to crystalline polymers are the crystallinity, crystal size, and crystal perfection, as well as preferential orientation caused by the oscillatory motion combined by squeeze flow under the action of normal force during welding process. This is the main focus of the present study.

MATERIALS AND EXPERIMENTAL PROCEDURES

Materials

Two PVDF-based materials were used, supplied by Elf Atochem North America, Inc. Figure 1 shows the repeating units of the polymers. The first is PVDF homopolymer (commercial name KYNAR-720), while the second is a random copolymer of PVDF with hexafluorpropilene (FMK) (commercial name KYNAR FLEX-2800). The comonomer (FMK) proportion is between 15–20% in weight.

Experimental procedures

Sample preparation

Rectangular parts of dimensions 62 × 2.5 × 6.5 mm were injection molded using a 85-ton Van Dorn using an end-gated cavity. The temperature profile used along the screw was set at 188, 204, and 221°C in both the end position and the die. The other processing parameters are: mold temperature: 40°C, holding pressure of 9.65 MPa (1400 psi) during the first 10 s, reducing it at 8.27 MPa (1200 psi) up to 20 s, and finally at 5.52 MPa (800 psi). The same processing conditions were used for both the homopolymer and copolymer. After the ejection, the molded pieces were hung on a wire to assure uniform cooling with air convection.

Using a band saw, the molded samples were cut into two equal halves having approximate dimensions 31 × 12.5 × 6.5 mm. To improve the welding repeatability, these cut surfaces were mounted on a special holder and cut surfaces were polished using a Buehler–Ecomet III polisher with #400 sandpaper.

Vibration welding machine

The vibration-welding machine (Fig. 2) consists of a hydraulic system to generate the vibratory motion, a pneumatic cylinder system to produce the normal force (pressure), and a sample holder mechanism. In addition, the machine is well equipped with sensors to detect the variables of the process.

The vibration welding parameters controlled during the process are: the frequency, amplitude, normal pressure and time. The welding time is chosen on the control panel by selecting the total number of cycles to be applied to the interface.

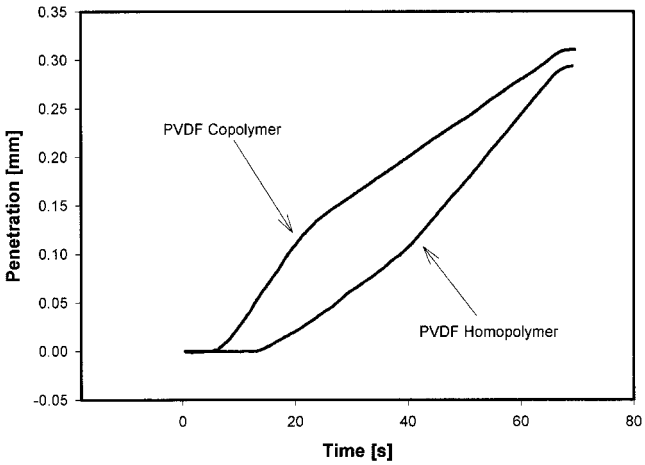

Figure 5 Penetration vs. time curves for homopolymer and copolymer.

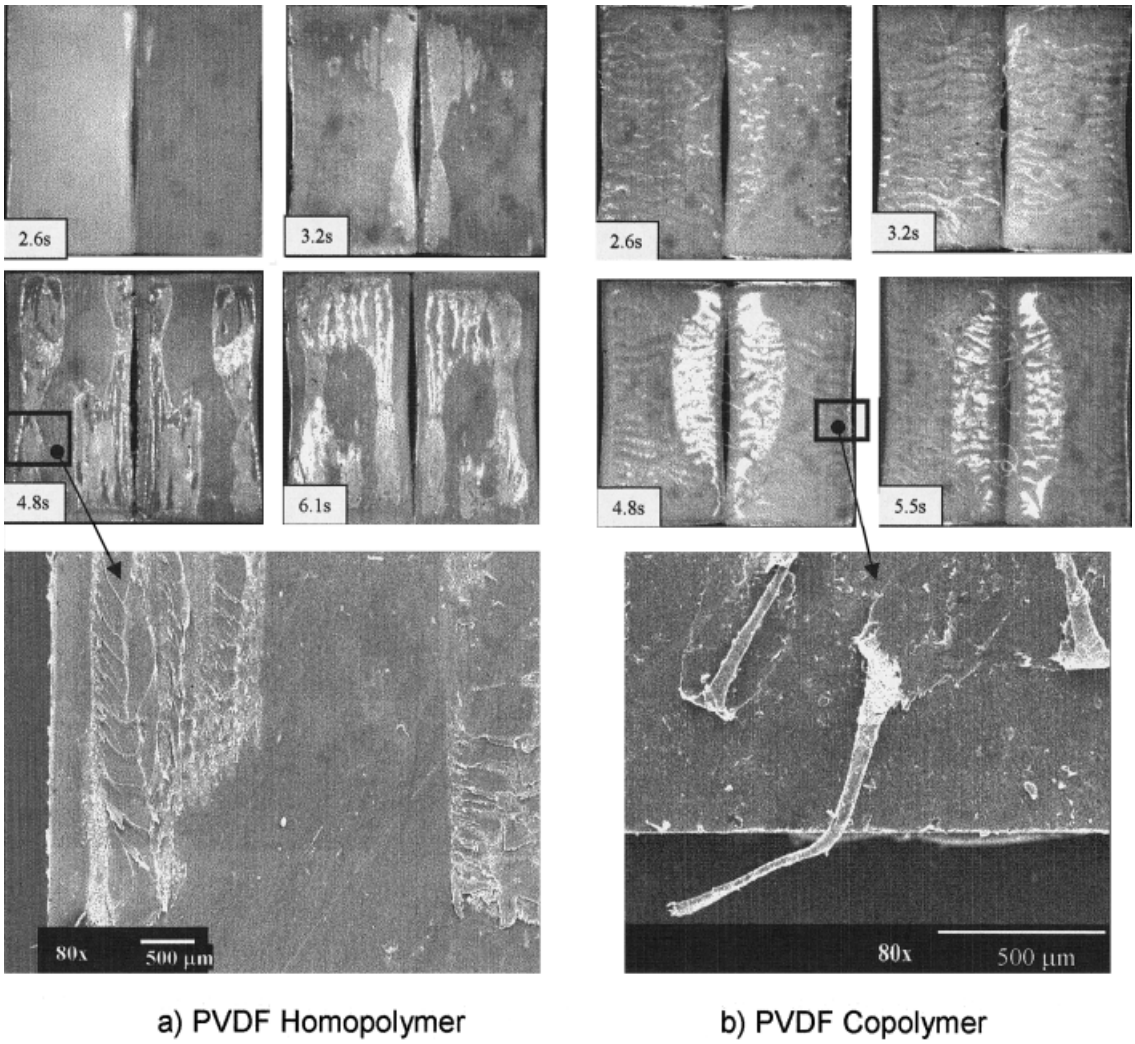

Figure 6 (a) PVDF homopolymer; (b) PVDF copolymer.

The weld penetration, which is the distance reduction of the two parts due to the material flowing outwards, was recorded using a Schaevitz LVDT 1000 HR sensor using a data acquisition system tailored to record all necessary parameters from the welding machine.

Time slicing

To study the material structure development during the vibration welding process, the experiments were carried out by stopping the process at a series of times keeping the rest of the parameters :frequency, amplitude, and pressure constant. The time intervals were kept shorter at the beginning of the process, as the most significant structural changes take place earlier in the welding process.

Regular industrial welding processes take place in very short times (e.g., 5 to 10 s) that makes the process difficult to be monitored. This is the reason to choose certain welding parameters (frequency: 60 Hz, amplitude: 0.85 mm, and normal pressure: 0.517 MPa to prolong the early welding period and be able to investigate the rapid structural changes that take place during the welding. Preliminary experiments were carried out covering a wide range of frequencies, amplitudes, and normal forces, including welding conditions close to the ones used in the industry. The experiments seemed to follow the same mechanism however the welding time was greatly affected.

Differential scanning calorimetry (DSC)

A Perkin-Elmer DSC7 was used to analyze the thermal behavior of the PVDF homopolymer and PVDF copolymer. Three different sections of the weld were used to obtain the samples. The first corresponds to the virgin-injected material. The second set of samples was obtained from the heat-affected material at the weld interface. The remaining samples were acquired from the fibers ejected from the interface. About 6 to 8 mg of material encapsulated in aluminum sample

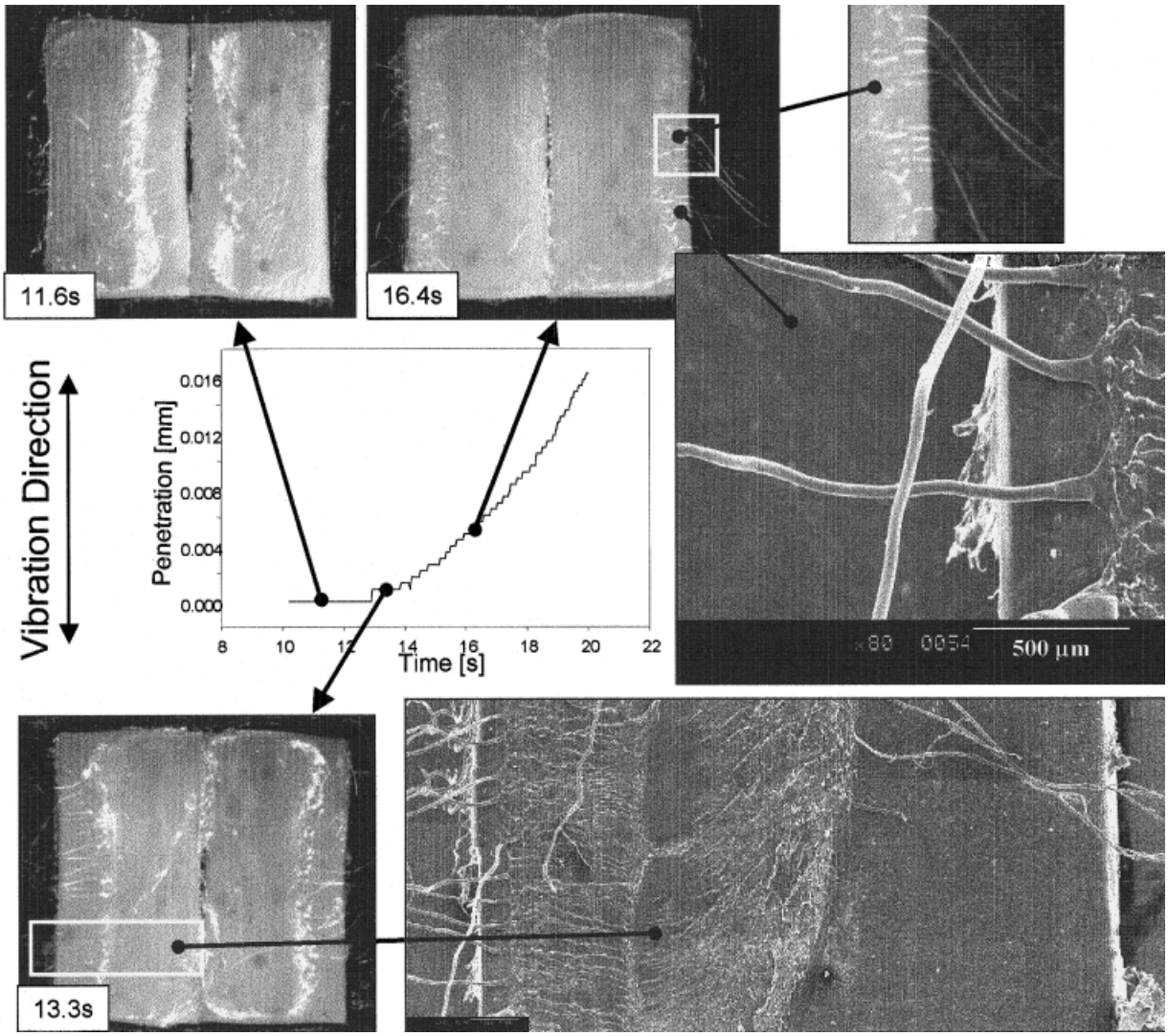

Figure 7 Surface topology of PVDF homopolymer during the second phase of the vibration welding process.

holders were scanned under dry nitrogen atmosphere from 50 to 200°C at a heating rate of 10°C/min.

Microscopy

Low magnification pictures of the weld interface were obtained using a 12-bit CCD-cooled camera with a 30° oblique lighting of the surface to create a good contrast.

For higher magnification pictures of the HAZ structural profile were obtained using a Leitz Laborlux 12 Pol-S optical microscope at 4× magnification. For this purpose, 200 μm-thick slices were cut in the X and Y directions shown in Figure 3 using a Buehler-Isomet low-speed diamond saw.

Scanning electron microscopy (SEM)

For selected observation of the fracture surface features and the produced fibrils, a Hitachi S-2150 SEM microscope was used operating at 20 kV and magnifications between 80× and 2000×.

For both polymers, micrographs at two different times of the process were taken; one corresponding to very short cycle times in the first phase of the vibration welding process, and the other corresponding to larger times at which substantial penetration had taken place. In addition, the material ejected outward by the normal pressure (fibers) was analyzed at cycle times of 8.7 and 16.4 s.

WAXS microbeam analysis

The 0.3 mm-thick samples were cut in two mutually perpendicular planes across the HAZ using a low-speed diamond saw following the previously described X-cut and Y-cut procedures shown in Figure 3. The micro-WAXS patterns were taken at 100-μm intervals starting well into the unaffected region and going across the HAZ to the other unaffected region

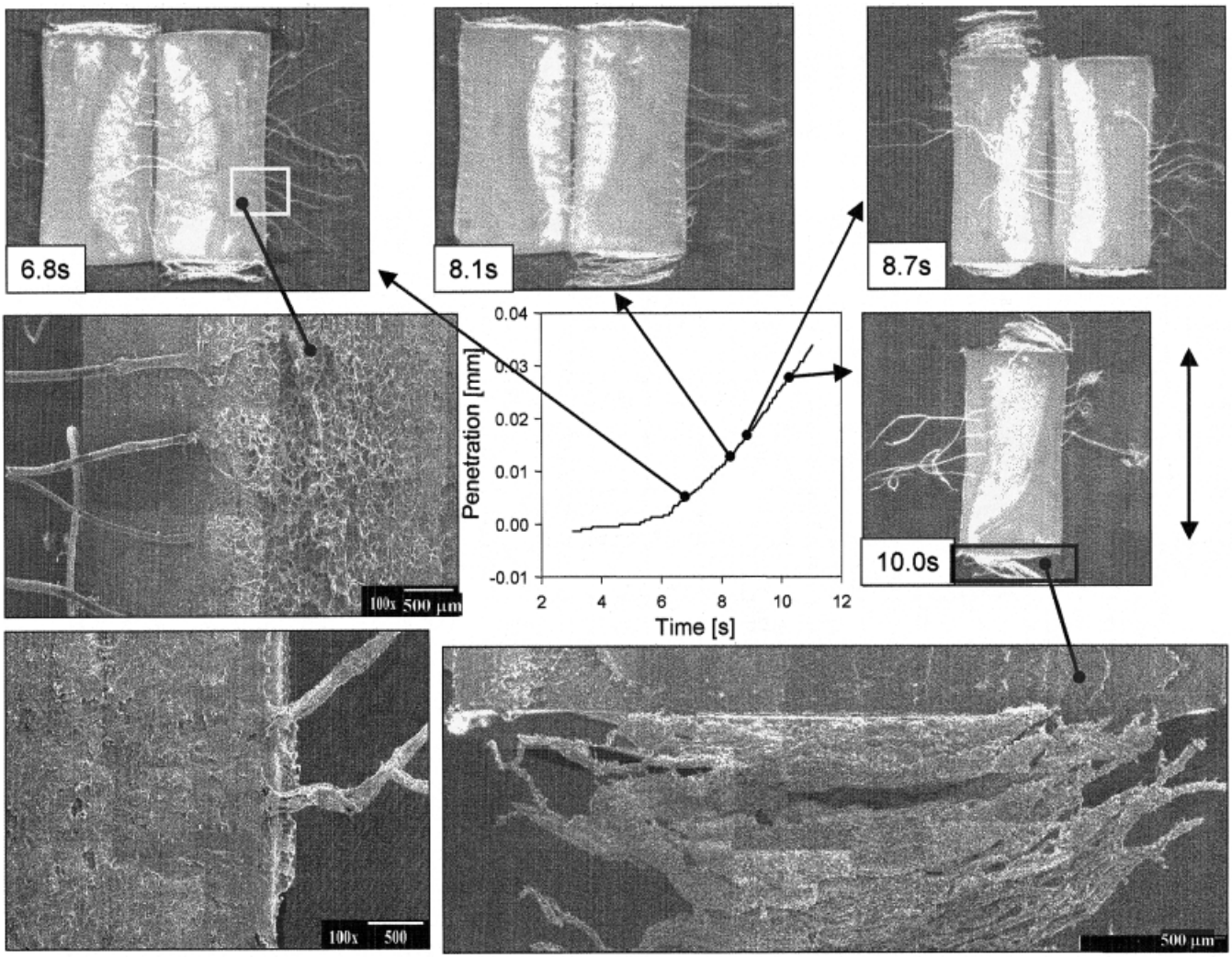

Figure 8 Surface topology of PVDF copolymer during the second phase of the vibration welding process.

using a specially constructed microbeam camera equipped with a precision X-Y stage sample holder. This camera was mounted on a Rigaku RU-200 12 KW X-Ray generator operated at 45 kV and 150 mA. The X-ray beam was monochromatized with nickel filter. Typical exposure times of about 2 h were used for each pattern.

RESULTS AND DISCUSSION

The differential scanning calorimeter scans of the two materials: PVDF homopolymer and PVDF copolymer used in this research are shown in Figure 4. As expected, the homopolymer shows substantially higher melting range (peak at 177.3°C) while the copolymer exhibits a much lower melting range due to the random inclusion of bulk hexafluorpropylene segments along the PVDF chain. As a result, the copolymer exhibits more elasticity than the homopopolymer.[20]

Penetration–time curves

Figure 5 shows the weld penetration curves for both the homopolymer and the copolymer for a frequency of 60 Hz, amplitude of 0.85 mm, and pressure of 0.517Mpa (75 psi). These weld penetration curves exhibit the four characteristic phases of the vibration welding process first discussed by Stokes.[5,6] As expected, because of the lower melting behavior of the copolymer, the Coulomb friction phase for the copolymer is shorter as the melting temperature is attained at a shorter time in comparison to the homopolymer. Also, the copolymer has a shorter second phase (17 s), and the penetration rate in this phase is higher in comparison to that of the homopolymer. These different penetration rates can be attributed to differences in the melt viscosity of the two polymers. The copolymer has a melt viscosity in the 22×10^3 and 27×10^3 poise range while homopolymer exhibits a lower viscosity in the 8×10^3 and 12×10^3 poise range.[20] The higher

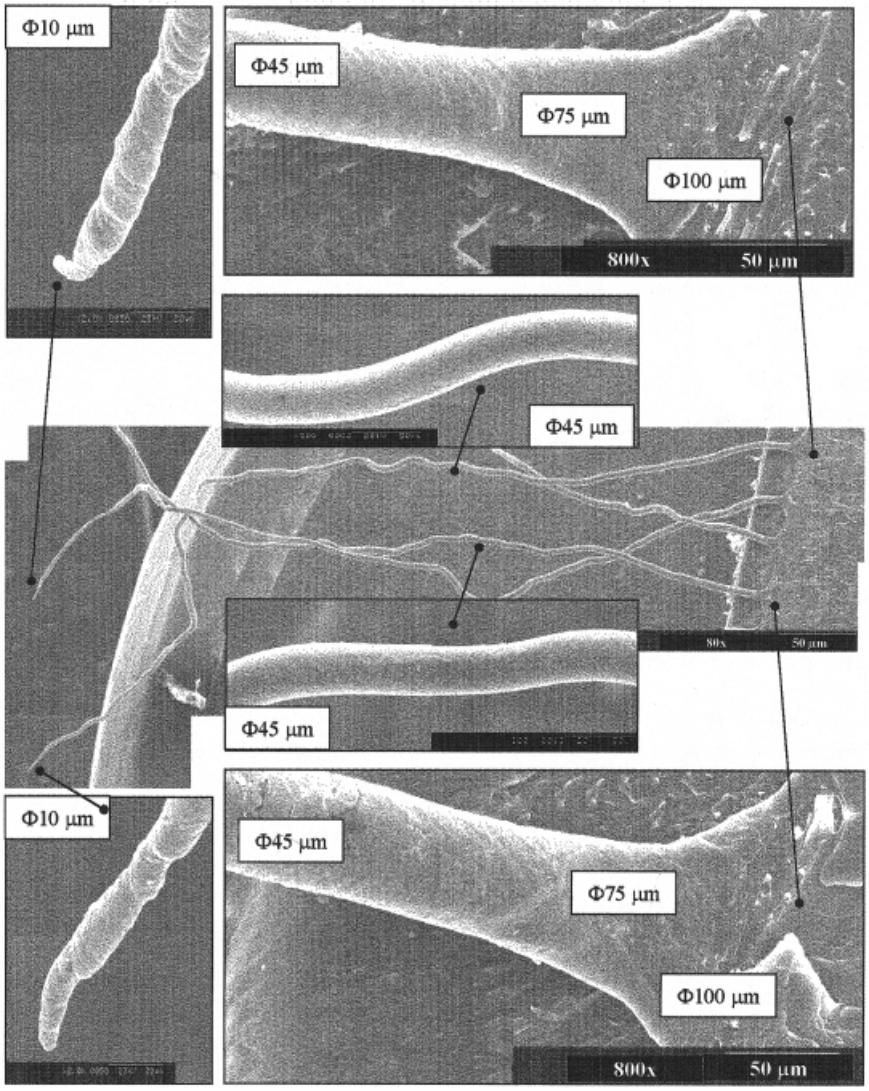

Figure 9 SEM monitoring of two PVDF homopolymer fibers formed at a welding time of 16.4 seconds (micrographs taken at the beginning, central part and at the end of the fiber).

viscosity of the copolymer molten layer material produces higher shear stresses as the parts are subjected to vibratory motion. The viscous dissipation, in turn, rises the temperature (shear heating proportionate to shear stress by shear rate square), resulting in a faster penetration rate. In the steady-state phase (third phase of the process), the larger slope of the PVDF homopolymer penetration–time curve results from the lower melt viscosity allowing the applied normal force to extrude out the melt from the interface more readily.

Although the vibratory motion is stopped in the fourth phase a small additional penetration is observed, which results from the extrusion of the molten material by the normal force that is applied in this phase.

Surface topology in heat-affected zone

Figure 6(a) and (b) show the weld surfaces during the first phase of the process for the homopolymer and the copolymer, respectively. In the localized rough areas on the initially smooth surface, melting start in isolated regions, initiated perhaps, by small asperities still remaining on the polished surfaces. These regions exhibit features elongated along the primary vibration direction, which is along the long axis of these samples. As melting progresses, these isolated regions coalesce with one another. At these times (2.6–6.1 s), no penetration was observed in Figure 5 and, consequently, no material is expelled from the interface.

The surface topology of the copolymer [Fig. 6(b)] is quite different from those shown in the homopolymer [Fig. 6(a)]. Initially, the formation of wave-like bands is observed with their long axes oriented normal to the vibration direction. The fractured brighter regions observed starting at a welding time of 4.1 s correspond to the fully fused portions of the interface obtained by fracturing the two pieces for observation. This also indicates that in this phase of welding the thickness of

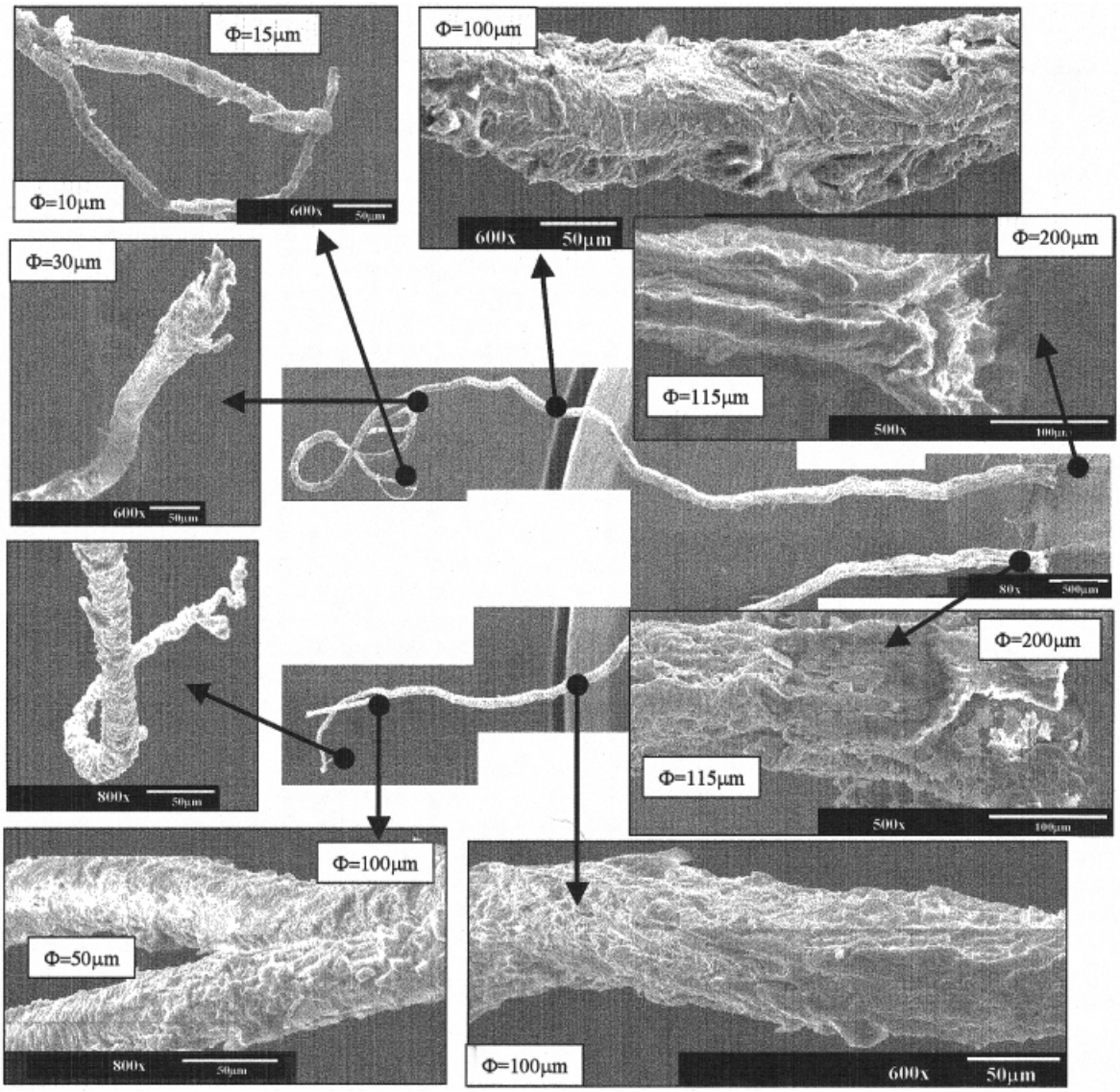

Figure 10 SEM monitoring of two PVDF copolymer fibers formed at a welding time of 16.4 seconds (micrographs taken at the beginning, central part and at the end of the fiber).

the molten layers varies along the wave-like bands being thickest at the crest and thinnest at the trough. Therefore, welding can take place at regions where the two crests of the waveforms spatially localize, increasing the probability for the molten polymer chains to interdiffuse across the interface to form a bond. These are the white fractured regions in these pictures.

The transition between the first and second phase of the welding process for the homopolymer can be observed in Figure 7. At 11.6 s, the friction affects the whole contact area and the beginning of the fiber formation can be observed. The amount of fiber produced increases with time and, at almost 16.4 s, this fiber production intensifies; this is reflected in the change of the slope of the penetration curves shown in Figure 5.

In the penetration–time curves, the weld penetration for the copolymer begins around 6 s. The surface topologies shown in Figure 8 indicate the formation of fiber-like structures. These fibers are extruded from the crests of the wave pattern observed in the first phase of the process.

Texture of the fibrillar extrudates

To understand the details of the formation of the fibers, an SEM study of the fibers was carried out for both materials (Figs. 9 and 10). The first figure shows two fibers corresponding to the homopolymer at 16.4 s at the beginning, the central part, and the end. The bases of the fiber have diameters of about 100 μm, which in a short distance decrease to 45 μm (this value remains along the rest of the fiber). Similar distances (about 400 μm) separate these structures and a smooth texture along its extension is observed. The fiber tips exhibit lower diameters (about 10 μm), as they were formed at the early stages of the process where the

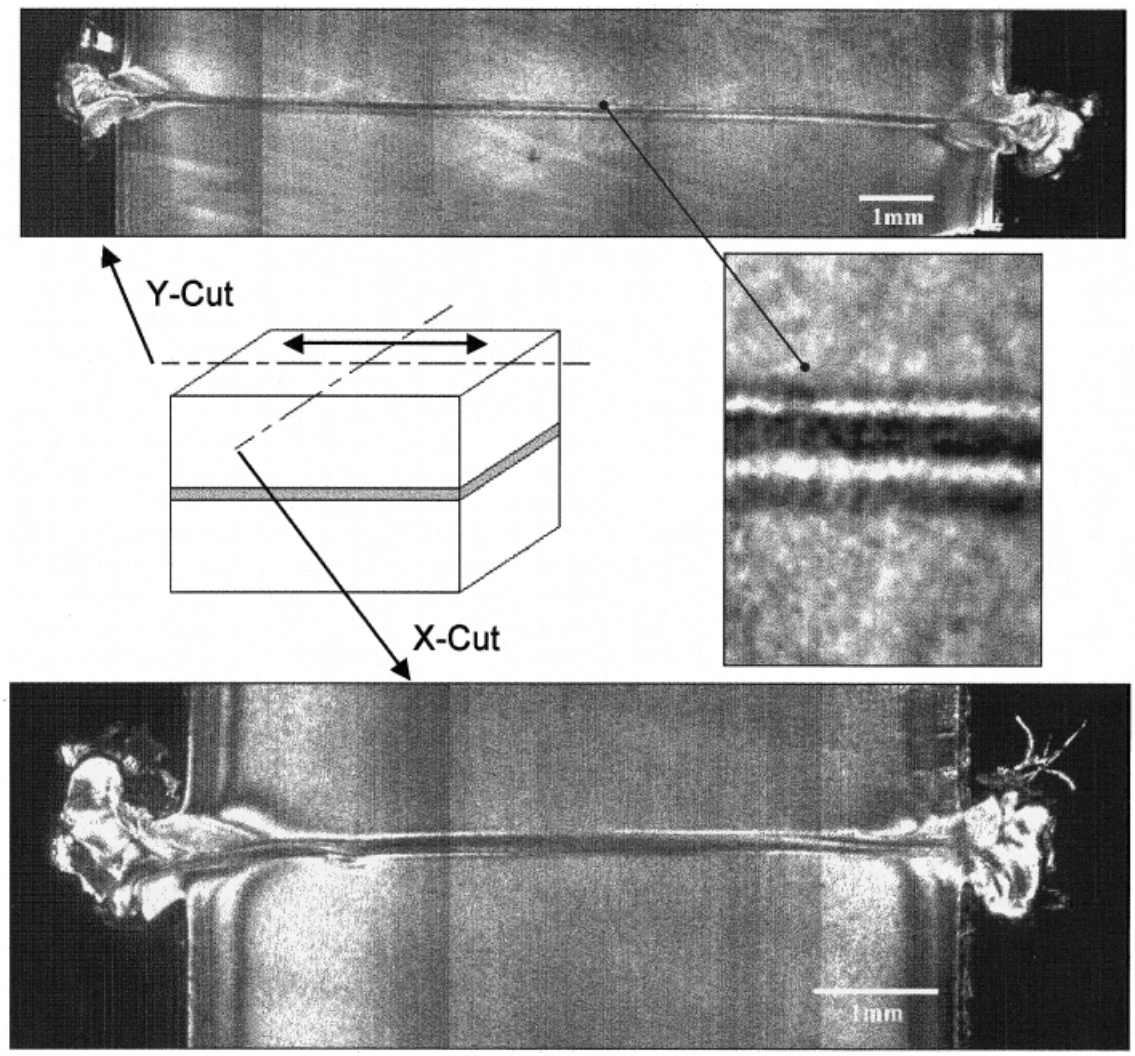

Figure 11 Optical micrographs across the HAZ of PVDF homopolymer samples welded at a vibration time of 65 s.

normal forces imparted on them would have been much larger due to the solid-solid friction.

Figure 10 shows the fiber development of the copolymer including the base, central part, and tip of two contiguous fibers. The fiber bases have diameters of about 200 μm, progressively decreasing to 100 μm. These diameters are twice as large as those observed in homopolymer. In contrast to the homopolymer, the surfaces of the fibers are very rough, attesting to significantly higher elasticity of the copolymer material. The tips of the fibers are bifurcated into two similar fibers having diameters of about 50 μm. This suggests that the copolymer fibers were formed out of a wave pattern similar to those observed in homopolymer, but unlike the homopolymer, the newly formed fibers of close proximity are joined together in the early stages of welding under the rolling action thereby creating such a tip.

Optical microscopy of the heat affacted zone

Figure 11 shows optical micrographs (under crosspolarized light) for the PVDF homopolymer samples at a vibration time of 65 s. The thickness of the HAZ is fairly constant in both directions, except at the edges where the HAZ is thicker. The larger HAZ thickness near the edges is directly related to the heating effect by the material that is transported from interior to the edges and accumulated at this location.

Figure 12 shows optical micrographs across the HAZ for the copolymer at 65.3 s. The vibration direction (Y-cut) exhibits a clear wave-like pattern, while the other direction (X-cut) has a flat interface with a higher thickness at the center, as expected.

Differential scanning calorimetry (DSC)

Figure 13(a) and (b) shows the heating DSC thermograms for injection molded bulk material, material taken out of heat affected zone, and collected fibers for both homopolymer and copolymer, respectively.

Both the injection-molded bulk and HAZ samples exhibit very similar behavior, but the fibers exhibit a lower peak melting position with broadening towards the lower temperature side. This is more

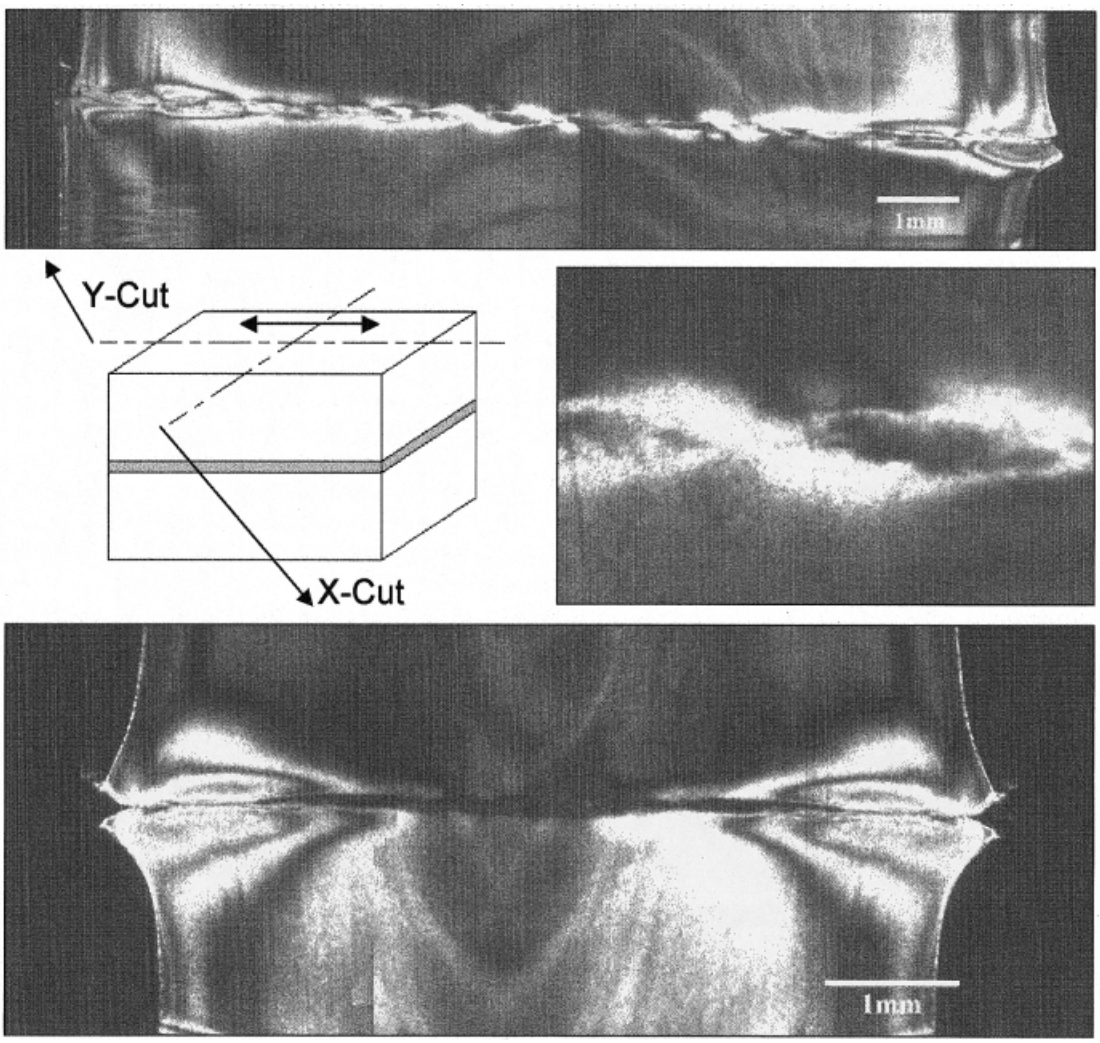

Figure 12 Optical micrographs across the HAZ of PVDF copolymer samples welded at a vibration time of 65 s.

pronounced in the homopolymer. For the homopolymer, the melting endotherms for the bulk and HAZ material exhibit a peak temperature of 177°C while that for the fiber is 172°C. The peak temperatures for the copolymer are 150 and 149°C, respectively. For both materials, the main reason for this difference is the presence of distorted crystalline structures in the fibers caused by the rapid convective cooling and rapid solidification as soon as they are expelled into the ambient air.

X-ray microbeam

WAXS X-ray microbeam was used to examine the state of the crystalline regions, including the molecular orientation along the HAZ. Figures 14(a) and (b) show the wide-angle X-ray patterns for the PVDF homopolymer taken with the X-ray beam directed normal to the vibration direction.

The characteristic monoclinic α form crystalline planes for PVDF can be observed in both figures, represented by four concentric crystalline diffraction rings belonging to (100), (020), (110), (021) of the α form starting from innermost proceeding outward.[21]

Remarkably, the microbeam X-ray patterns indicate no preferential orientation development in the crystalline regions. The WAXS patterns taken with the X-ray beam along the vibration direction (not shown) also exhibit no orientation. This suggests that any orientation developed by the oscillatory motion at the interface during welding relaxes prior to solidification in the HAZ. This is in accord with earlier studies on PVDF spin welding where preferential crystalline orientation was not observed.[21] In contrast, poly(ethylene naphthalate) exhibited substantial preferential orientation in the vibration direction.[18]

The micro-WAXS results on the copolymer samples shown in Figure 14(b) also confirms the behavior observed in homopolymer samples. Note that in these patterns the crystalline rings are more diffuse compared to those of the homopolymer, indicating

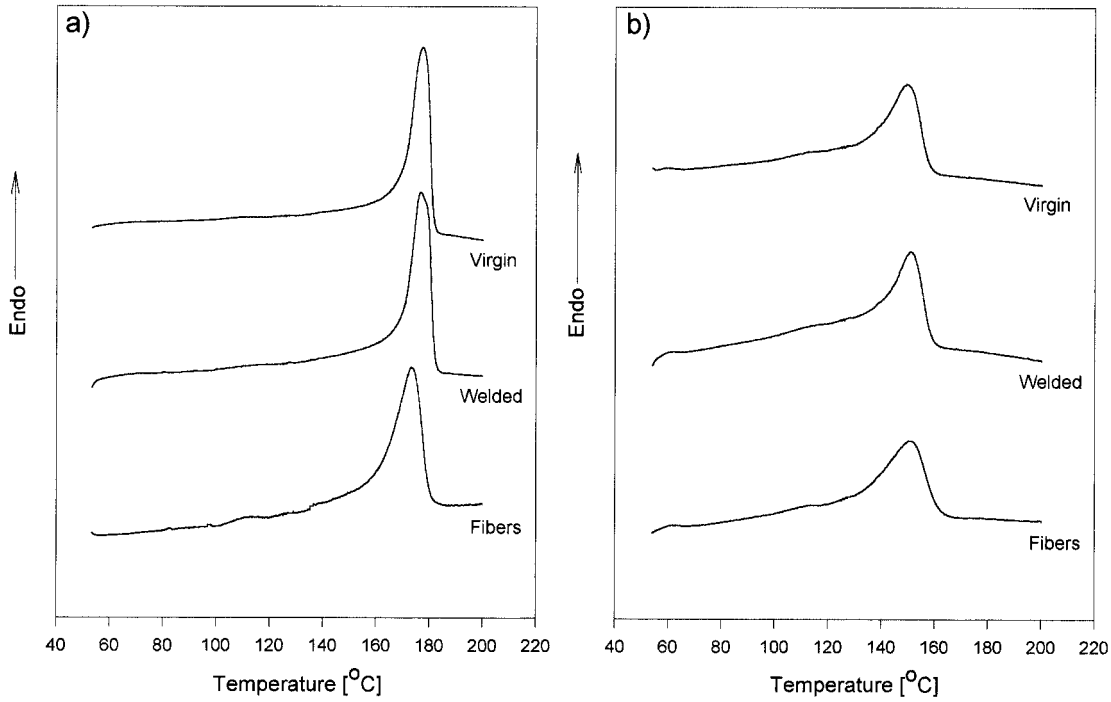

Figure 13 Heating DSC thermograms for bulk material, material taken out from the HAZ, and collected fibers. a) PVDF homopolymer; b) PVDF copolymer.

the presence of higher levels of crystalline distortions and/or smaller crystallites in the copolymers.

CONCLUSIONS

In the homopolymer and the copolymer studied, welding starts in isolated regions with their long axes oriented in the vibration direction. These regions grow in size until they coalesce to cover the entire interface of the pieces being welded (Fig. 15). The copolymer, having much higher elasticity, goes through this process in a rather unique way by forming wave patterns with the wave normals along the vibration direction. This mechanism is much less pronounced in the homopolymer. The thickness of the wave pattern increases with increasing welding time.

In both materials, the extrusion of the material from the interface does not occur as a uniform squeezing flow, but occurs as fibrillar extrusions from the crests of the wave patterns caused by the rolling action of the welding process.

The WAXS X-ray microbeam patterns show no preferential molecule orientation along the HAZ. The high elasticity and mobility of the polymeric chains causes

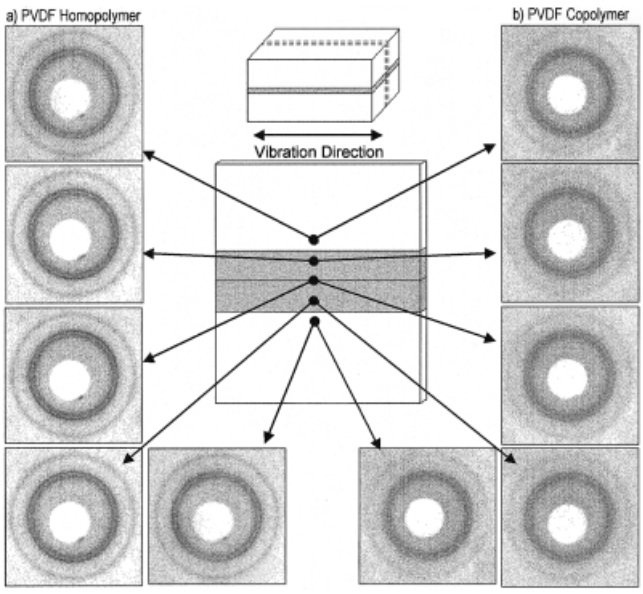

Figure 14 WAXS microbeam X-ray along the HAZ. a) PVDF homopolymer; b) PVDF copolymer.

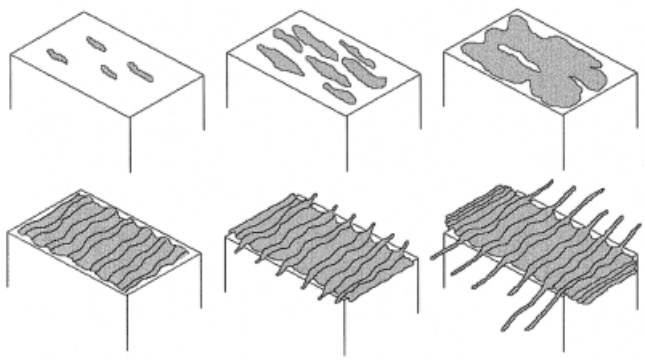

Figure 15 Basic stages of the welding process.

any orientation developed during the vibration to be lost before the material solidifies.

The results described above suggest that the welding process is more complicated than that assumed in earlier mathematical modeling studies. Semicrystalline polymers of high-melt elasticity exhibit completely different patterns initiating from interfacial instabilities caused by the severe oscillatory shear flow in the welding process.

One of us (D.V.) would like to acknowledge Dr. Cristian Puig for his encouragement during this research.

References

1. Stokes, V. K. Polym Eng Sci 1989, 29, 1310.
2. Gallagan, S. T. SPE Antec Tech Papers 1985, 850.
3. Bauer, L. Weld Des Feb 1990, 72–75, April.
4. Tappe, P.; Potente, H. Polym Eng Sci 1989, 29, 1655.
5. Stokes, V. K. J Mater Sci 1988, 23, 1772.
6. Stokes, V. K. Polym Eng Sci 1988, 28, 989.
7. Stokes, V. K. Polym Eng Sci 1988, 28, 998.
8. Stokes, V. K. Polym Eng Sci 1989, 29, 1683.
9. Schlarb, A.; Ehrenstein, W. Polym Eng Sci 1989, 29, 1677.
10. Giese, M.; Ehrenstein, W. SPE Antec Tech Papers 1992, 349.
11. Potente, H.; Natrop, J.; Klit, M.; Uebbing, M. J Thermoplast Compos Mater 1993, 6, 147. Also SPE Antec Tech Papers 1993, 2075.
12. Froment, I. D. SPE Antec Tech Papers 1995, 1285.
13. Stokes, V. K. SPE Antec Tech Papers 1993, 2067.
14. Kagan, V, Lui, S.-Ch.; Smith, G. R. SPE Antec Tech Papers 1996, 1266.
15. Stokes, V. K.; Hobbs, S. Y. Polym Eng Sci 1989, 29, 1667.
16. Stokes, V. K.; Hobbs, S. Y. Polymer 1993, 34, 1222.
17. Cakmak, M.; Robinette, J. SPE Antec Tech Papers 1997, 1627.
18. Cakmak, M.; Robinette, J.; Schaible, S. J Appl Polym Sci 1998, 70, 89.
19. Barnhart, W. S.; Hall, N. T. Encyclopedia of Chemical Technology, 2nd ed. 1990, 9, 840.
20. Kynar and Kynar Flex PVDF Technical Brochure; Elf Alochem North America, Inc., 1998.
21. Schaible, S.; Cakmak, M. Int Polym Process 1995, 10, 270.